# Optimal Location Area Design to Minimize Registration Signaling Traffic in Wireless Systems

Erdal Cayirci, *Member*, *IEEE*, and Ian F. Akyildiz, *Fellow*, *IEEE*

**Abstract**—In this paper, a new scheme is developed for optimal location area design in wireless systems. New algorithms based on intercell traffic prediction and traffic-based cell grouping are used to select the optimal set of cells for location areas (LAs). The expected intercell movement patterns of mobiles are determined by using the new intercell traffic prediction algorithm. Further, the cells are partitioned into LAs by applying the new traffic-based cell grouping algorithm where the cell pairs with higher intercell mobile traffic are grouped into the same LA. Hence, the inter-LA mobile traffic is decreased by increasing the intra-LA mobile traffic. Experimental results show that this cell grouping algorithm reduces the number of location updates by 27 percent to 36 percent on average compared to proximity-based cell grouping schemes.

**Index Terms**—Location area design, traffic-based location area design, location update, registration, paging, cellular wireless systems.

## 1 Introduction

In cellular wireless networks, the location information about a mobile is maintained by registration [1], [13] where mobiles update their location area (LA) information in the home location register (HLR). An LA is a set of cells and may be static or dynamic. A static LA is comprised of a group of cells that are permanently assigned to the LA and is fixed for all mobiles. On the other hand, dynamic LAs are created for each mobile during a registration process. Although signaling traffic can be reduced by using dynamic LAs [3], [4], [6], [10], [11], they impose higher computation and separate data storage of LAs for each mobile. As a result, most of the current cellular systems use static LAs.

Both in static and dynamic LA designs, determining the optimal number of cells in each LA is important and challenging. The number of cells in an LA plays a substantial role in the signaling traffic, which is composed of paging and registration traffic in location management. With a trade off, when the number of cells in an LA is high, the registration traffic decreases, but the paging traffic [2], [12], [15] increases. On the other hand, for smaller LAs, the registration traffic increases, but the paging traffic decreases. Overall, an optimal number of cells in an LA reduces the location management signaling traffic significantly. Therefore, most of the recent references related to the location area design are focused on how to determine an optimal number of cells for an LA. Models that capture the trade off between the traffic created by paging and registration are proposed in [5], [7], and [14]. Another formulation to find the optimal number of cells in an LA and to design global LAs for one-dimensional cellular networks is proposed in [9].

The number of cells in an LA is not the sole factor affecting the location management signaling traffic. If the cells are partitioned into LAs without considering the expected intercell mobile traffic, increasing the number of cells in an LA may also increase the registration traffic, as well as the paging traffic. Hence, the cell-partitioning technique is also very important. If the LAs are designed such that the inter-LA mobile traffic is reduced, the registration traffic decreases for the same LA size.

In this paper, instead of determining the optimal number of cells in an LA as in [5], [7], [9], [14], we focus on selecting the optimal set of cells for each static LA. We use the intercell traffic prediction and traffic-based cell grouping schemes consecutively to partition the cells into LAs. The intercell traffic prediction scheme is applied to determine the expected intercell movement patterns of mobiles. The total number of intercell movements of mobiles can be predicted by examining the roads (highways, carriageways, footpaths, etc.) between neighbor cells. These predictions are used by the traffic-based cell grouping scheme to group cells into LAs. The neighbor cells with higher intercell traffic are assigned to the same LAs. Hence, the inter-LA movements of mobiles are decreased by increasing the intra-LA movements. The inter-LA movements of mobiles create registration traffic. Therefore, we can reduce signaling traffic by increasing the intra-LA movements of mobiles.

The remainder of the paper is organized as follows: In Section 2, we describe the static location area design (LAD) without considering the intercell mobility patterns, namely, *the proximity-based LAD*. In Section 3, we introduce our new scheme for static location area design where LAs are created based on the expected intercell mobile traffic. Further, we

• *The authors are with the Broadband and Wireless Networking Laboratory, School of Electrical and Computer Engineering, Georgia Institute of Technology, Atlanta, GA 30332. E-mail: {erdal, ian}@ece.gatech.edu.*

*Manuscript received 15 Oct. 2001; revised 27 Sept. 2002; accepted 19 Jan. 2003.*
*For information on obtaining reprints of this article, please send e-mail to: tmc@computer.org, and reference IEEECS Log Number 8-102001.*

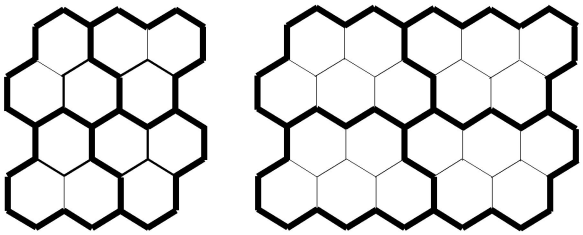

Fig. 1. Cell clustering patterns for three and five cell LAs.

introduce an intercell traffic prediction scheme, an optimal traffic-based LAD model, and an approximation algorithm for optimal traffic-based LAD. We give experimental results in Section 4. Finally, we conclude the paper in Section 5.

## 2 Proximity-Based Static Location Area Design

In the static LAD, the cells in a service area are partitioned into fixed LAs. While a mobile is moving from one of these fixed LAs to another, it reports its new LA by a registration process. Since every mobile uses the same LA partitioning for registration, this design paradigm is called *static LAD*.

The cells can be grouped into static LAs based on proximity. This is called *proximity-based static LAD* (PB-LAD). The cell clustering patterns, as shown in Fig. 1, can be used to partition the cells into proximity-based LAs. In Fig. 1, the cells are represented by hexagons and the borders of LAs are illustrated by bold lines. If the cells do not have fixed size and are not regularly spaced as in Fig. 1, a regular pattern may not be used to design static LAs. In that case, the cells close to each other are grouped into LAs such that all of the cells belong to one and only one LA.

In Fig. 2, five-cell static LAs are created by using the PB-LAD technique where the road map of a region is covered by a fixed size hexagonal cell layout. In the road map, different types of lines are used for representing different types of roads, such as dashed lines for secondary carriageways, solid lines for primary carriageways, and solid bold lines for highways. Each hexagon represents a cell and bold lines along the cell borders separate the LAs. In Fig. 2, if a mobile moves between points $a$ and $b$ following the highway, it crosses the LA borders six times. Hence, this mobile needs to register six times when we use PB-LAD to design LAs for the cells given in Fig. 2.

## 3 Traffic-Based Static Location Area Design

Our new solution, called *the traffic-based static LAD* (TB-LAD), is to group cells according to the expected intercell mobility patterns. The objective of the TB-LAD is to design static location areas for a given LA size such that the inter-LA movements of mobiles are minimized. This is achieved by grouping the cell pairs with higher intercell mobile traffic into the same LA. Hence, the inter-LA mobile traffic is decreased by increasing the intra-LA mobile traffic. Formally, we define TB-LAD as follows:

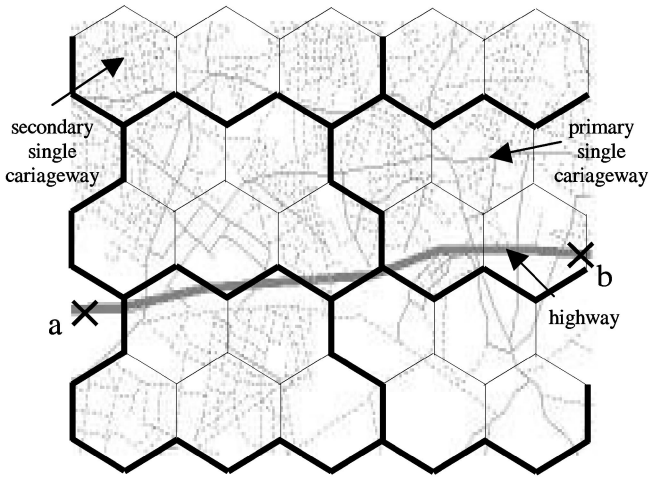


Fig. 2. Proximity-based static location area design.

**Definition (TB-LAD).** *Given a set of cells $S = \{c_1, c_2, \ldots, c_m\}$, a set of intercell traffic densities $I = \{t_{01}, t_{02}, \ldots, t_{ij}\}$, and the maximum number $\eta_{max}$ of cells for an LA, partition $S$ into a family of disjoint subsets $F = \{S_1, S_2, \ldots, S_k\}$ such that the cardinality of each member in $F$ is lower than or equal to $\eta_{max}$, and the total expected intercell traffic densities between the members of each subset in $F$ is maximized.*

The same scenario in Fig. 2 is also used to explain how the TB-LAD reduces the number of inter-LA movements. When we determine LA borders by using our scheme TB-LAD, the borders of location areas are modified as shown in Fig. 3. The mobile moving between points $a$ and $b$ crosses an LA boundary only once when the new LA borders are used. This is six times less than the number of LA border crossings of the mobile in the PB-LAD case as shown in the previous section. Since many mobiles may be on the highway, it is obvious that the number of inter-LA movements is reduced drastically by modifying LA borders as proposed in Fig. 3.

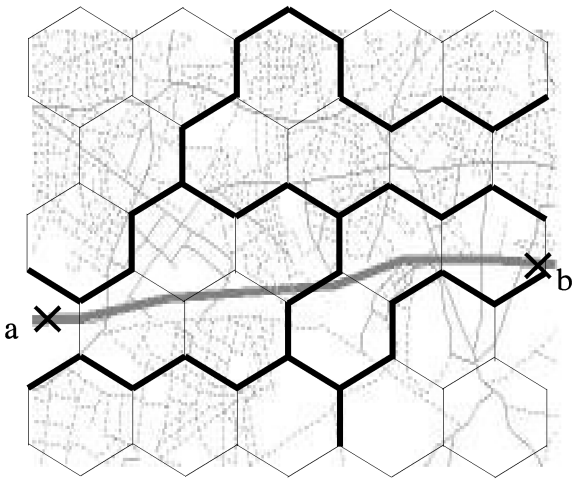


Fig. 3. Traffic-based static location area design.

TABLE 1
An Example Traffic Density Multiplication Factor Look Up Table

| Type \ Surface | Loose Surface | All Weather | Asphalt | Concrete |
|---|---|---|---|---|
| Footpath | - | 0.016 | - | - |
| Sea Route | - | 0.2 | - | - |
| Railroad | - | 5 | - | - |
| Single Carriageway | 0.033 | 0.2 | 6 | 6 |
| Dual Carriageway | 5 | 20 | 20 | 20 |
| Highway | 5 | 30 | 30 | 30 |

### 3.1 The Intercell Traffic Prediction

The first step for the TB-LAD is to determine the expected amount of mobile movements between the pairs of cells as accurately as possible. Since mobiles generally move on roads (e.g., paths, streets, railroads, highways, etc.), we can use roads to predict intercell roaming patterns of mobiles. These predictions can be used as the expected intercell traffic for the TB-LAD. The expected traffic $t_{kij}$ from cell $i$ of LA $k$ to its neighbor cell $j$ of LA $k$ is computed from

$$t_{kij} = \sum_{z=1}^{r_{kij}} d_{kijz}, \tag{1}$$

where

- $d_{kijz}$ is the traffic density of road $z$ between cell $i$ of LA $k$, and cell $j$ and
- $r_{kij}$ is the total number of roads between cell $i$ of LA $k$ and cell $j$.

We can determine the traffic density $d_{kijz}$ of each road by observing the traffic. These observations must be carried out for a long period of time, e.g., a year, for accurate prediction because mobility patterns may vary by season, month, days of the week, and by several other factors. Since the observation of traffic densities for a long period of time and for a large number of roads may be impractical, we need to develop a model to predict the potential traffic density of a road based on its characteristics.

We use type and surface characteristics of a road to build the so-called *density multiplication factor look up table*. A *density multiplication factor* is the number of vehicles expected per unit of time on a single lane of a road. Table 1 is an example of a *density multiplication factor lookup table* created by observing the traffic during rush hour in our experiment region. Note that the network operators can use different scales for types and surfaces of roads and they may have different *multiplication factor lookup tables* for different cities according to the regional observations.

We can obtain the traffic density $d_{kijz}$ of a road by using density multiplication factors:

$$d_{kijz} = m_{kijz} \cdot s_{kijz}, \tag{2}$$

where

- $m_{kijz}$ is the density multiplication factor of road $z$ between cell $i$ of LA $k$ and cell $j$, and
- $s_{kijz}$ is the number of lanes of road $z$ between cell $i$ of LA $k$ and cell $j$.

The advantage of using (2) to predict the expected intercell traffic is that there exists already digitized road data for many cities and metropolitan areas. Apart from road data, only traffic density multiplication factors are needed in (2).

### 3.2 Optimal Traffic-Based Location Area Design

The objective of our new TB-LAD scheme is to design LAs such that the number $\beta_m$ of inter-LA movements of the mobiles is minimized. The expected inter-LA traffic $\beta_t$ can be predicted by using the road data:

$$\beta_t = \sum_{k=1}^{l} \sum_{i=1}^{\eta_k} \sum_{j \in S'_k} t_{kij}, \tag{3}$$

where

- $t_{kij}$ is traffic between cell $i$ of LA $k$ and cell $j$,
- $S'_k$ is the set of cells which are not members of LA $k$,
- $\eta_k$ is the number of cells in LA $k$, and
- $l$ is the number of LAs.

In order to minimize $\beta_t$, we maximize the expected intra-LA area traffic $\varphi_t$ determined from

$$\varphi_t = \sum_{k=1}^{l} \sum_{i=1}^{\eta_k} \sum_{j \in S_k} t_{kij}, \tag{4}$$

where $S_k$ is the set of cells which are members of LA $k$.

Our objective function is

$$\text{maximize } \varphi_t \tag{5}$$

subject to

$$1 \leq \eta_k \leq \eta_{max} \quad \text{for } k = 1, \ldots, l,$$

where

- $\eta_k$ is the number of cells in LA $k$ and
- $\eta_{max}$ is the maximum number of cells in an LA.

**Lemma.** *By maximizing $\varphi_t$, we minimize registration-signaling traffic.*

**Proof.** The total number $\phi$ of cell boundary crossings is the sum of intercell movements $\varphi_m$ between the cells of the same LA and interlocation area movements $\beta_m$. Therefore, we can express $\beta_m$ as

$$\beta_m = \phi - \varphi_m. \tag{6}$$

Since $\varphi_t$ is the expected $\varphi_m$ and $\beta_m$ decreases when $\varphi_m$ increases, as shown in (6), we can minimize $\beta_m$ by maximizing $\varphi_t$. The inter-LA movements of mobiles create registration traffic. Therefore, we can minimize registration traffic by maximizing the $\varphi_t$ that is the condition in the lemma. □

### 3.3 The Approximation Algorithm for Traffic-Based LAD

In this section, we first prove that the optimal TB-LAD problem stated in the beginning of this section is NP-complete

and then introduce an algorithm that approximates the optimal solution.

**Theorem.** *Optimal TB-LAD under the condition of the maximization of intra-LA traffic is NP-complete.*

**Proof.** We can represent an instance for the recognition version of the optimal TB-LAD problem with five tuples ($l$, $[\eta_k]$, $[T_k]$, $\eta_{max}$, $T$), where the set of number of cells in each LA $[\eta_k]$ and the set of intra-LA traffic for each LA $[T_k]$ have $l$ members, which is the number of LAs, $\eta_{max}$ is the maximum number of cells in an LA, $T$ is a value that represents minimum feasible number of total intra-LA movements, and $T_k$ can be determined by

$$T_k = \sum_{i=1}^{\eta_k} \sum_{j \in S_k} t_{kij}, \tag{7}$$

where $t_{kij}$ is traffic between cell $i$ of LA $k$ and cell $j$.

Since a polynomial algorithm can check whether all values in $[\eta_k]$ satisfy the constraint $1 \leq \eta_k \leq \eta_{max}$ and whether $\Sigma T_k \geq T$, this problem is a member of NP. Hence, it will suffice to show that an NP-complete problem polynomially transforms to the optimal TB-LAD problem. We use the *3-exact cover problem* [8], that is, "*Given a family* $F = \{S_1, \ldots, S_n\}$ *of n subsets of*

$$S = \{u_1, \ldots, u_{3m}\},$$

*each of cardinality 3, is there a subfamily of m subsets that covers S*." It is proven in [8] that the 3-exact cover problem is NP-complete.

First, we transform the subsets in $F$ to the strings of *1*s and *0*s of length $3m$. For instance, Subset $S_1 = \{u_2, u_4, u_6\}$ of $S = \{u_1, u_2, u_3, u_4, u_5, u_6\}$ becomes $V_1 = 010101$ and Subset $S_2 = \{u_1, u_4, u_5\}$ of the same set becomes $V_2 = 100110$. Then, we combine all strings into a single string as $V_f = V_1 + \ldots + V_n$, where + is the logical "*or*" operation and $V_f$ is the final string. We complete transformation by the following assignments: The cardinality of $S$, which is $3m$, is assigned to the number of LAs (i.e., $l = 3m$). We create a set of 3s with $3m$ members for $[\eta_k]$, which indicates $3m$ LAs that have exactly three cells. Each bit in the final string $V_f$ becomes a member of $[T_k]$. The maximum number $\eta_{max}$ of cells in an LA and the minimum total intra-LA traffic $T$ are written as 3 and $3m$, respectively (i.e., $\eta_{max} = 3$ and $T = 3m$). Since this is a polynomial time transformation of the 3-exact cover problem to the optimal TB-LAD and the 3-exact cover problem returns *TRUE* if and only if the recognition version of the optimal TB-LAD problem returns *TRUE* for the transformed case, it proves the theorem. □

Since the optimal TB-LAD problem is NP-complete, we designed the algorithm in Fig. 4. This algorithm reaches a feasible solution which is the approximation of the optimal TB-LAD for a given topology.

Using the approximation algorithm in Fig. 4, we first create a list of neighbors for each cell. The neighbor lists are ordered according to the predicted traffic between the neighbor cells and the list heads, i.e., the cell for which the neighbor list is created. Then, we order these lists according to the traffic between the list heads and the first neighbors in the lists. Before creating the first LA, we initialize all of the list heads as "*NOT INCLUDED*." A loop iterates until all of the cells are included. In each iteration, the first "*NOT INCLUDED*" cell from the cell list is selected and a new LA is created with this cell. Then, an inner loop finds neighbors with the highest predicted traffic from the neighbor lists of the cells that are included for the current LA and includes them into the current LA. The inner loop terminates when there is no neighbor that can be included or the maximum number of cells is reached for the current LA.

```
1. Create a list of neighboring cells for each
cell. The list of neighboring cells must satisfy t_{i,m}
≤ t_{i,m+1} where t_{i,m} is the traffic from cell i for which
the list is prepared, to its neighbor m in the list.
2. Create an ordered list of cells in which t_{i,1} ≤
t_{i+1,1} where t_{i,1} is the traffic between the cell i in
the list and the first cell in its list of
neighboring cells.
3. Initialize all cells as 'NOT INCLUDED'.
4. Initialize current LA number i.
                    i←1
5. Repeat until there is no cell that is 'NOT
INCLUDED'.
   5.1. Construct a new LA a_i.
   5.2. Initialize the number l_{ai} of cells for a_i.
                    l_{ai}←1
   5.3. Include the highest ordered 'NOT INCLUDED'
cell c_{1ai} from the cell list.
   5.4. Mark c_{1ai} as 'INCLUDED'.
   5.5. Repeat until there is no more cell which is
in the neighbors list of one of the cells included
for a_i and 'NOT INCLUDED' or l_{ai}>η_{max}.
      5.5.1. Find a new 'NOT INCLUDED' cell c_{new} with
highest t_{m,cnew} from the neighbor lists of the cells
included for a_i.
      5.5.2. Include c_{new} into a_i.
      5.5.3. Mark c_{new} as 'INCLUDED'.
      5.5.4. Increment l_{ai}.
                    l_{ai}←l_{ai}+1
   5.6. Increment i.
                    i←i+1
```

Fig. 4. The approximation algorithm.

## 4 Experimental Results

We compare the performance of TB-LAD and PB-LAD by using two sets of experiments. In the first set of experiments, we digitize all types of roads in a real metropolitan area from a scanned hardcopy map. We use a vector format to store the road data where each road is represented by a sequence of grid coordinates. We also keep some additional information such as the type, the surface type, and the number of lanes of the road about each road in our data structures. This road data can be downloaded from our Web site [16]. Note that, for the road and the surface types, we use the scales given in Table 1. After digitizing the roads of the metropolitan area, we create cells for the area by using a fixed size hexagonal layout. Then, we run both TB-LAD and PB-LAD techniques to design the LAs. Finally, we calculate the expected inter-LA traffic for the LAs designed by two approaches and compare them.

In the second set of experiments, we interviewed 56 people living in the same metropolitan area. The interviewed people have different professions where 26 of

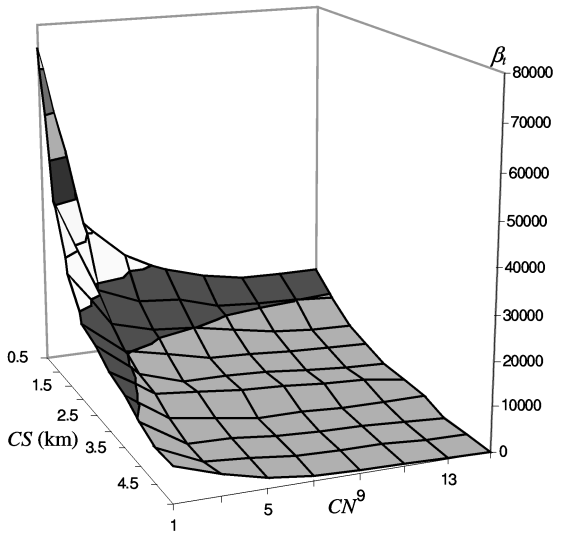


Fig. 5. Expected interlocation area traffic for TB-LAD.

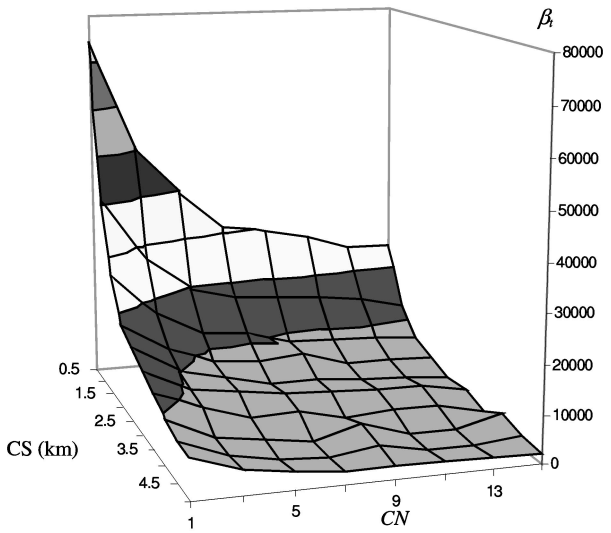


Fig. 6. Expected interlocation area traffic for PB-LAD.

them are sales people, 22 of them are office workers (academicians, managers, etc.), and eight of them are housewives. These people have different mobility characteristics. For instance, sales people are frequently on the road and office workers generally stay in their offices during daytime in the week. Through these interviews, we determined the places that the people had visited in the previous week. Then, we stored this information as a sequence of grid coordinates and times in a data structure similar to the one used for the road data. In the second type of experiments, we trace the movements of the interviewed people by using these mobility data on the LAs designed by TB-LAD and PB-LAD and count the number of inter-LA movements, then compare the results.

### 4.1 The Expected Inter-LA Traffic

We carried out both TB-LAD and PB-LAD schemes on the digitized road data of the metropolitan area. After the completion of LA designs, we calculated the expected inter-LA traffic $\beta_t$ by using (3).

The results of the experiments are given in Figs. 5 and 6, where $CS$ and $CN$ axes represent the cell size in kilometers and the number of cells in an LA, respectively. Color codes are used to illustrate the change in $\beta_t$. By examining these color codes, the difference in $\beta_t$ between Figs. 5 and 6 can be observed.

In Fig. 5, $\beta_t$ decreases as $CS$ or $CN$ becomes higher. The smoothness of the surface indicates that the increase in $CS$ or $CN$ always leads to a decrease in $\beta_t$. As shown in Fig. 6, the decrease in $\beta_t$ is not as smooth as in Fig. 5, which means we cannot guarantee reducing $\beta_t$ by increasing $CS$ or $CN$ when PB-LAD is used. We will examine the reasons in detail later.

In Fig. 5, we observe a 57 percent decrease of $\beta_t$ when we modify $CN$ from 1 to 3. For $CN = 1$, each LA has a single cell. Therefore, the addition of the first two cells to the LAs decreases $\beta_t$ by more than half. As shown in Fig. 6, in PB-LAD, addition of the first two cells reduces 32 percent of $\beta_t$, which is less then the decrease in the TB-LAD case. The improvement achieved by TB-LAD can be seen by examining the color codes used in Figs. 5 and 6.

The ratio $\delta_t$ of the difference between the $\beta_t$ of PB-LAD and TB-LAD to the $\beta_t$ of PB-LAD is shown in Fig. 7. We do not observe any negative $\delta_t$ in Fig. 7, which means TB-LAD always performs better. TB-LAD reduces 36 percent of $\beta_t$ over PB-LAD on the average. For the case of having one cell in each LA, $\delta_t$ is always zero. For large $CN$ and $CS$ values, TB-LAD outperforms PB-LAD. $\delta_t$ becomes almost 1 for $CS = 5$ km and $CN = 15$. For $\delta_t = 1$, there is no $\beta_t$ for TB-LAD. In our experiments, for $CS = 5$ and $CN = 15$, the proposed approximation algorithm for TB-LAD can manage to divide the region into two LAs between which the traffic density is almost zero.

In Fig. 8, the cross sections of Figs. 5 and 6 are taken on the $CS$ axis for $CN = 11$. For both TB-LAD and PB-LAD, $\beta_t$ becomes higher when $CS$ is modified from 2.5 km to 3 km. When the cell size increases, the cellular layout changes,

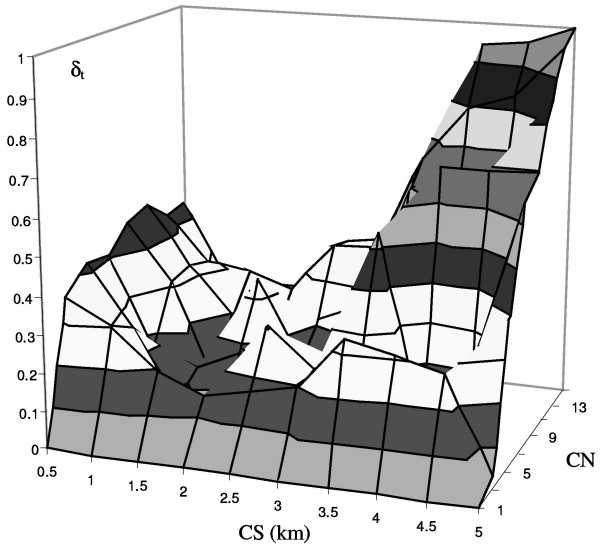


Fig. 7. Expected interlocation area traffic change ratios.

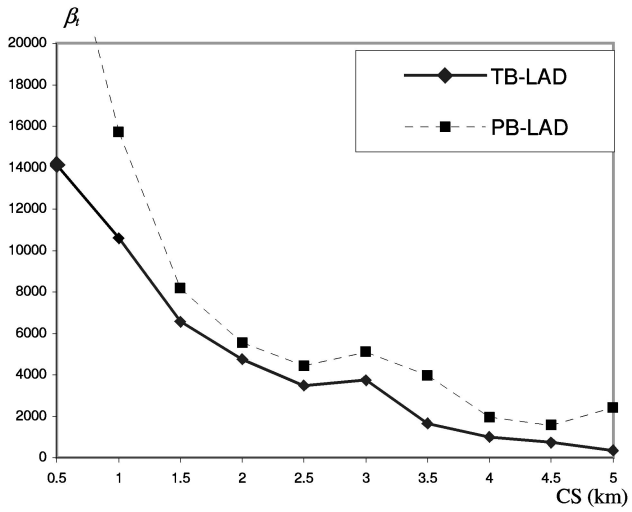


Fig. 8. Expected interlocation area traffic for $CN = 11$.

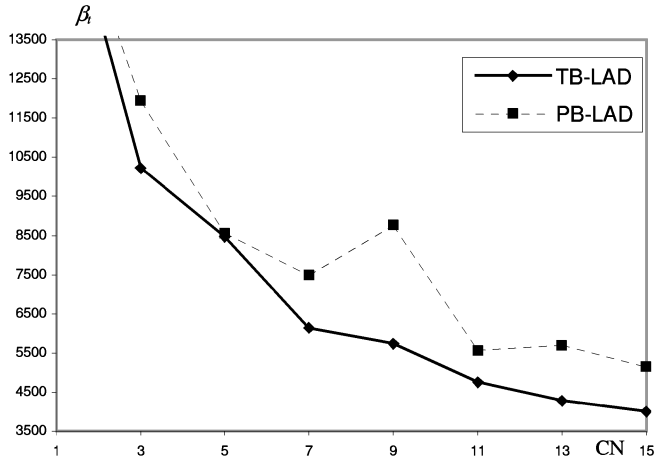


Fig. 10. Expected interlocation area traffic for $CS = 2$ km.

where the cell borders can then become very close to the roads with high traffic. Since a road along a cell border may often pass back and forth between the neighboring cells, the inter-LA traffic $\beta_t$ increases. Note that, under normal conditions, increasing the cell size would reduce $\beta_t$.

In Fig. 9, $\delta_t$ values for the cross sections in Fig. 8 are shown. For $CS = 2$ km, $\delta_t$ reaches the lowest value. For the smaller and larger $CS$s, $\delta_t$ becomes higher. There is a sudden $\delta_t$ increase for $CS = 3$ km. The reason for this is the increase in $\beta_t$ for PB-LAD, for $CS = 2.5$ km and $CS = 3.5$ km, which is explained in the previous paragraph. This increase in $\beta_t$ for PB-LAD makes $\beta_t$ for PB-LAD two times larger than $\beta_t$ for TB-LAD at $CS = 3.5$ km. Consequently, a sudden increase in $\delta_t$ is observed for $CS = 3.5$ km.

In Fig. 10, cross sections of Figs. 5 and 6 are taken on the $CN$ axis for $CS = 2$ km. There should not be any increase in $\beta_t$ when $CN$ becomes larger because the cell layout does not change by modifying $CN$. However, we observe such an increase for PB-LAD when $CN$ is modified from 7 to 9. Since we apply fixed patterns in PB-LAD without any intercell traffic consideration, increasing $CN$ may sometimes make the cells with lower intercell traffic group into the same LAs. Grouping the cells with lower intercell traffic into the same LAs increases $\beta_t$. On the other hand, increasing $CN$ always decreases $\beta_t$ for TB-LAD. This also indicates that the results of changing $CN$ in TB-LAD are more predictable.

### 4.2 Inter-LA Movements of Interviewed Mobile Users

After we designed LAs by using TB-LAD and PB-LAD techniques for the road data of the experiment area, we traced the mobility patterns of the interviewed people and count each of the inter-LA movements. $\beta_m$ is the total number of inter-LA movements counted for all of the interviewed people. In Figs. 11 and 12, $\beta_m$ values are shown for different $CS$ and $CN$ values. Observations made in these figures are similar to those made in Figs. 5 and 6.

The $\beta_m$ values in Fig. 12 are higher than in Fig. 11, which indicates that PB-LAD performs worse than TB-LAD. There is a significant improvement achieved by our new scheme TB-LAD in particular for higher $CS$ and $CN$ values.

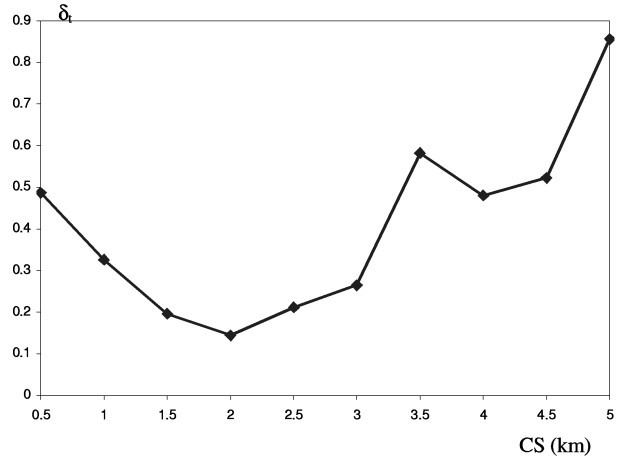


Fig. 9. Expected interlocation area traffic change ratios for $CN = 11$.

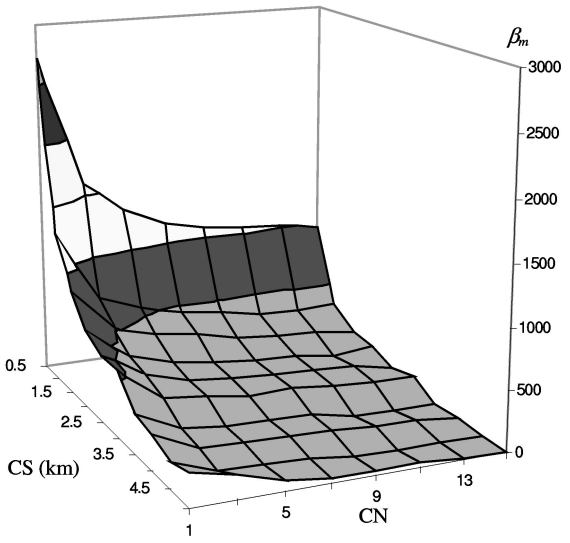


Fig. 11. Number of interlocation area movements for TB-LAD.

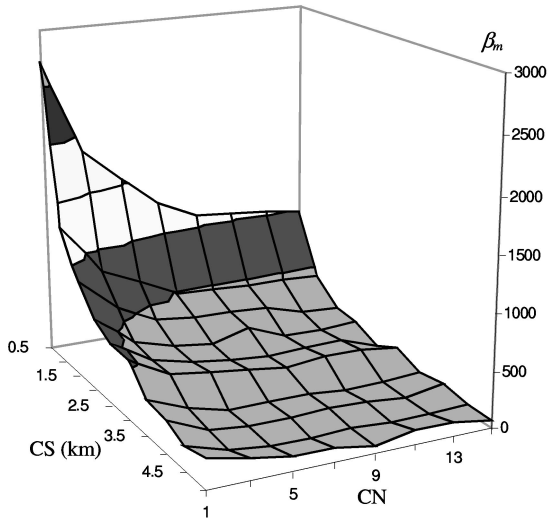


Fig. 12. Number of interlocation area movements for PB-LAD.

The inter-LA movement change ratios $\delta_m$ are given in Fig. 13. Similarly to $\delta_t$, $\delta_m$ gives the improvement in $\beta_m$ made by TB-LAD over PB-LAD.

As shown in Fig. 13, our scheme, TB-LAD, always performs better than PB-LAD and decreases $\beta_m$ 27 percent on the average. The improvement of TB-LAD is more significant in larger $CN$ and $CS$ values.

The cross sections of Figs. 11 and 12 are given in Figs. 14 and 15. Although increasing $CS$ normally reduces $\beta_m$ as shown in Fig. 14, $\beta_m$ becomes higher as we increase $CS$ for $CS = 2.5$, 3, or 4 km in PB-LAD and for $CS = 4$ km in TB-LAD. When we modify the cell size, the cell layout changes. Even if we enlarge the cells, this may increase the total intercell traffic because some of the highways may fall in the border of a cell when $CS$ becomes larger, which, in turn, increases the total $\beta_t$. Hence, higher traffic is shared among the LAs and $\beta_m$ becomes higher. We make similar observation in Fig. 8.

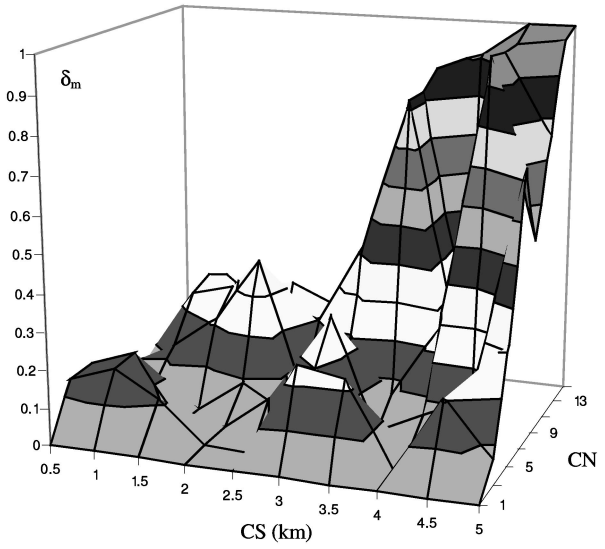


Fig. 13. Interlocation area movement change ratios.

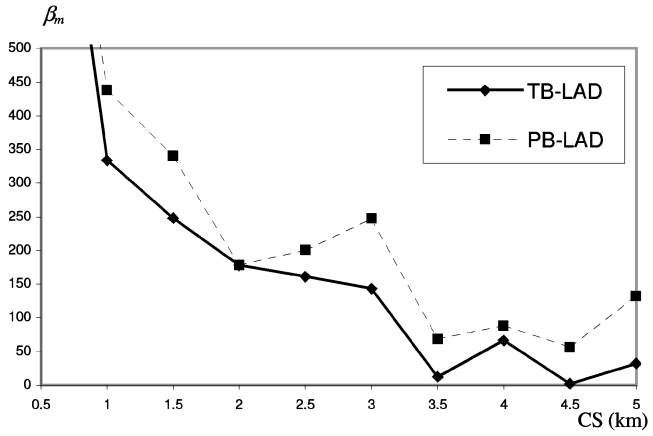


Fig. 14. Number of interlocation area movements for $CN = 11$.

The effect of modifying $CN$ value is more predictable for TB-LAD, as shown in Fig. 15. TB-LAD always reduces $\beta_m$ for higher $CN$, where $\beta_m$ increases in some cases for PB-LAD. Since the PB-LAD is not based on predicted traffic, LA patterns may be shifted such that major roads may fall in the LA borders for increasing CN values, which in turn increases $\beta_m$.

We evaluate the performance of TB-LAD also for a more realistic cellular design where the cell sizes may vary and the cells may overlap. We use a cell layout similar to the layout used by the operators in our experiment region, where cell sizes are less than 1,000 meters in densely populated areas and around 3,000 meters along the less densely populated highways in urban areas. The results from the experiments carried out on this realistic cell layout by using our real mobility traces are shown in Fig. 16. The relation of $\beta_m$ to CN for the more realistic case is similar to the one for the hexagonal cell layout case. However, $\delta_m$ for the realistic design is 0.47 on the average, which is 0.2 higher than the hexagonal design. This means that the TB-LAD performs better when realistic cell sizes and locations are used in our experiment region. Since the cell sites are selected based on population density and roads, the performance gain of the TB-LAD scheme becomes higher in realistic cellular design cases.

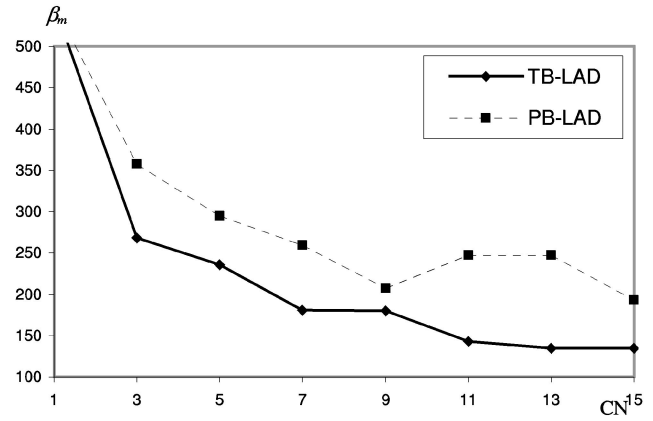


Fig. 15. Number of interlocation area movements for $CS = 3$ km.

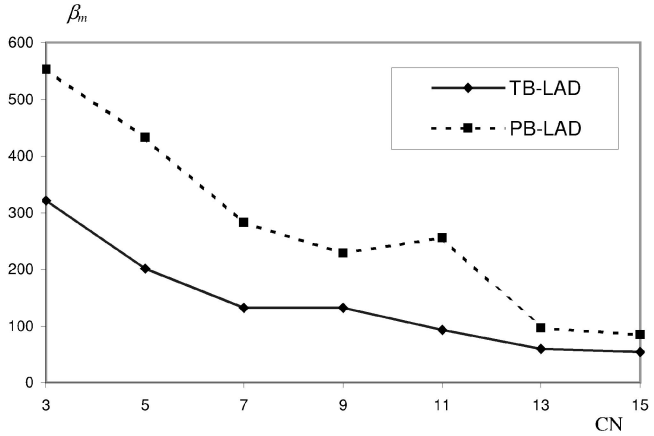


Fig. 16. Number of interlocation area movements for a realistic cell layout.

### 4.3 The Optimal Solution

In Table 2, we compare the optimal design solution with the results of the approximation algorithm. We make a taboo search on a tree to find the optimal LAD solution, which is the maximization of the objective function (5). Each node of the tree has $l$ (the number of LAs) children and depth $n$ (the number of cells). Although we stop searching a branch as soon as we detect that the branch is infeasible during a depth first traversal of the tree, the complexity of such a search is $O(l^n)$. Therefore, we did not find the optimum solution for every experiment.

For $CS = 4,500$, the total number of cells required to cover the experiment region is 24. We optimized this cellular layout for $CN = 15$ and $CN = 13$ in which we need only two LAs. For $CS = 5,000$, 20 cells are enough to cover the region. For 20 cells, we searched the optimal solutions for two, three, and four LAs. When there are two LAs, our approximation algorithm given in Fig. 4 always reaches the optimal solution. As shown in Table 2, when there are three LAs, the approximation algorithm misses the optimal solution in one of two cases. However, the result of our approximation algorithm is very close to the optimal one in case it misses the optimal solution. We think that the difference between the optimal solutions and the results of the approximation algorithm becomes larger when the number of LAs increases because the increasing number of LAs reduces $\delta_t$, as shown in Fig. 7. The reduction in $\delta_t$ means that the difference between the results of the TB-LAD and the PB-LAD decreases. This may indicate that our approximation algorithm does not reach the optimal solution for a high number of LAs. Nevertheless, our intuition is that they start to get closer again after a point as CN decreases (i.e., for $CN = 2$ and $CN = 3$), because we observe that $\delta_t$ increases again in that region. As illustrated in Table 2, TB-LAD always outperforms PB-LAD for large CN and CS values.

TABLE 2
Comparison of the Approximated Results with the Optimal Solutions

| CS | total # of cells | CN | total # of LAs | $\beta_t$ optimum | $\beta_t$ TB-LAD | $\beta_t$ PB-LAD |
|---|---|---|---|---|---|---|
| 4500 | 24 | 15 | 2 | 104 | 104 | 2525 |
| 4500 | 24 | 13 | 2 | 262 | 262 | 1571 |
| 5000 | 20 | 15 | 2 | 0.2 | 0.2 | 2319 |
| 5000 | 20 | 13 | 2 | 76 | 76 | 2425 |
| 5000 | 20 | 11 | 2 | 349 | 349 | 2425 |
| 5000 | 20 | 9 | 3 | 700 | 818 | 2702 |
| 5000 | 20 | 7 | 3 | 855 | 855 | 2425 |
| 5000 | 20 | 5 | 4 | 2272 | 2272 | 3717 |

TABLE 3
Traffic Density Multiplication Factor Look Up Table

| Surface Type | Loose Surface | All Weather | Asphalt | Concrete |
|---|---|---|---|---|
| Footpath | - | 0.016 | - | - |
| Sea Route | - | 0.2 | - | - |
| Railroad | - | 0.05 | - | - |
| Single Carriageway | 0.033 | 0.5 | 0.8 | 0.8 |
| Dual Carriageway | 0.05 | 1 | 1 | 1 |
| Highway | 0.05 | 1.3 | 1.3 | 1.3 |

### 4.4 The Sensitivity of the Traffic Density Multiplication Factor

In this section, we examine how sensitive the TB-LAD technique is to the changes in traffic density multiplication factors given in Table 1. We run all experiments for the second time by using the factors in Table 3. The differences among the factors in Table 3 are not as large as the differences among the factors in Table 1. For instance, the traffic density multiplication factor is 1.3 for a concrete highway and 0.8 for a concrete single carriageway in Table 3. The multiplication factor for a highway is only 1.625 times larger than the multiplication factor for a single carriageway. For the same example, the multiplication factor for a highway is five times larger than the multiplication factor for a single carriageway in Table 1.

After changing multiplication factors, we do not observe much difference in the $\beta_t$-$CN$-$CS$ and $\beta_m$-$CN$-$CS$ relations for TB-LAD and PB-LAD. The major differences occur in the $\delta_t$ and $\delta_m$ values. After applying the new traffic density multiplication factors, both of the average $\beta_t$ and $\beta_m$ reductions made by TB-LAD over PB-LAD become 24 percent. The average $\beta_m$ reduction is very close to the one obtained by applying the multiplication factors in Table 1. However, the $\beta_t$ reduction for the case in Table 3 is 11 percent less than the $\beta_t$ reduction for the case in Table 1.

In Fig. 17, we show $\delta_t$ values for the multiplication factors in Table 3. This figure differs from Fig. 7 by the following: When the differences between the traffic density multiplication factors are high, the approximation algorithm can group the cells along the same major roads like highways and dual carriageways into same LAs. This makes the results of TB-LAD closer to the optimal solutions, which means more reduction in $\beta_t$. Therefore, the average $\delta_t$ is lower in Fig. 17.

We also observe that the $\delta_t$ values for lower $CS$ in Fig. 7 are higher than the $\delta_t$ values in Fig. 17. For lower $CS$, the

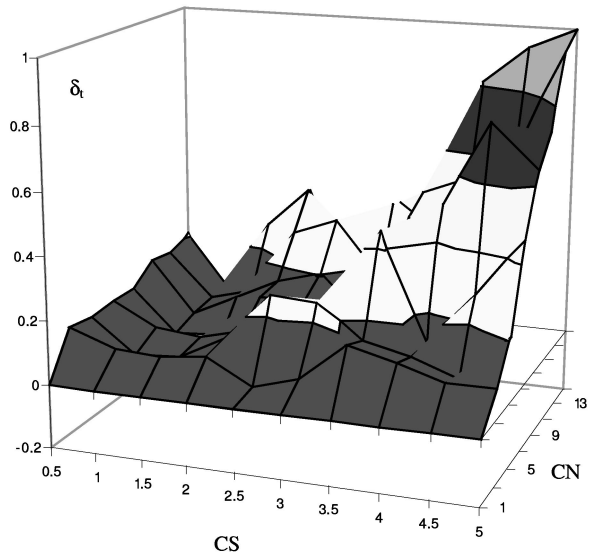


Fig. 17. $\delta_t$ for the multiplication factors in Table 3.

total number of cells needed to cover the experiment region increases. The average distance between the optimal solutions and the results of the approximation algorithm becomes larger when the differences between the multiplication factors are not large and the total number of cells is high. When the difference between the results of the approximation algorithm and the optimal LAD solutions is high, the results of PB-LAD are closer to those of TB-LAD.

Although it is not visible in Fig. 17, our most critical observation related to $\delta_t$ is the presence of negative $\delta_t$ values that indicates PB-LAD may perform better. For $CN = 9$, $\delta_t$ is -0.00052 for $CS = 1$ and -0.02257 for $CS = 1.5$. Since the approximation algorithm cannot guarantee the optimal solution, it is possible to reach a better LAD by using a regular pattern. This is independent of the traffic density multiplication factors. The PB-LAD technique may reach a better LAD when the approximation algorithm does not reach the optimal solution.

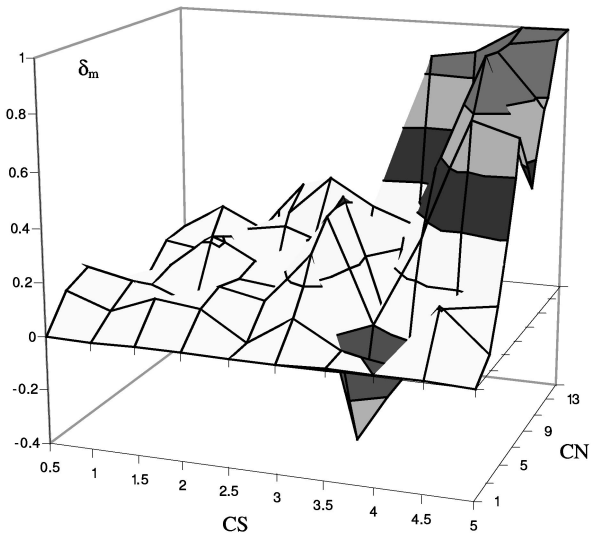


Fig. 18. $\delta_m$ for the multiplication factors in Table 3.

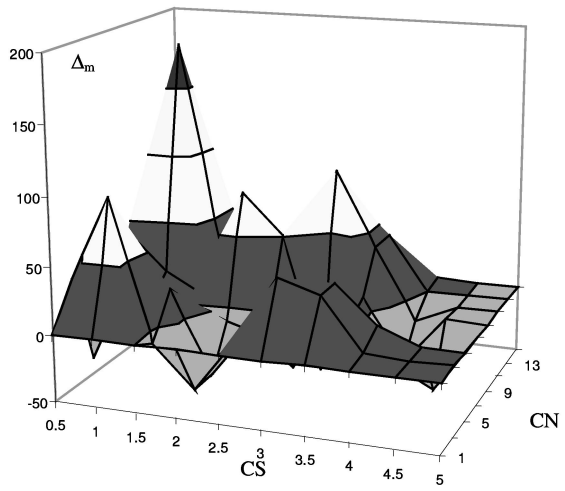


Fig. 19. The change in $\delta_m$ for the change in multiplication factors.

In Fig. 18, we show $\delta_m$ values for the multiplication factors in Table 3. The observation in Fig. 18 is the same as in Fig. 17. The main difference is in the number of negative values. The ratio of negative $\delta_m$ values is 15 percent. This means that the PB-LAD technique performs better in 12 out of 80 experiments when we use the traffic density multiplication factors in Table 3. However, TB-LAD still reduces $\beta_m$ 24 percent on the average compared to PB-LAD.

In Fig. 19, we illustrate the difference $\Delta_m$ between $\beta_m$ values for the multiplication factors in Tables 3 and 1. These $\beta_m$ values are determined by using the approximation algorithm. If $\Delta_m$ is negative, it indicates that the approximation algorithm performs better with the multiplication factors in Table 3. The ratio of negative $\Delta_m$ values is 26 percent. The multiplication factors in Table 3 increase $\beta_m$ 7.225 on the average. We can conclude that the approximation algorithm performs better when we increase the differences among the traffic density multiplication factors.

## 5 Conclusion

In static LAD, the cells of a cellular wireless network are partitioned into LAs where an LA is comprised of a group of cells that are permanently assigned to the LA and fixed for all mobiles. A mobile crossing an LA border registers its new LA. When there is an incoming call for the mobile, the cells in the last registered LA are paged. The number of cells in an LA is the major factor that constitutes the number of registrations and paged cells. Therefore, most of the recent references [5], [7], [9], [14] related to the location area design are focused on how to determine the optimal number of cells for an LA. In these papers, it is assumed that the registration traffic decreases and the paging traffic increases for larger LAs. However, increasing the number of cells does not always decrease the registration cost if the cells are grouped into LAs without considering that the mobility traffic between cells is different for each cell pair. This is clearly observed in our experiments. When we design LAs based on only proximity, we observe that the number of location updates may increase for higher LA sizes. In our experiments, we also observe that designing LAs based on

expected intercell mobile movements significantly decreases inter-LA mobile movements.

Being motivated by this, we developed the TB-LAD scheme where we first predict the mobile traffic between the cells based on the characteristics of roads traversing them. Then, using these traffic expectations, the traffic-based cell grouping technique partitions cells into LAs such that the neighbor cells with higher intercell traffic are assigned to the same LAs. Since the number of cells in an LA is not a changing parameter in TB-LAD, it does not increase or decrease the paging traffic. However, better design of an LA, i.e., partitioning cells into LAs based on predicted intercell movements of mobiles, reduces the number of location updates. Therefore, TB-LAD decreases the number of location updates without increasing the number of paged cells during a call delivery.

To evaluate the performance of our new scheme, we performed experiments by using data collected in a metropolitan area. We examine the relation of inter-LA traffic with cell size and number of cells in an LA and compare the performance of our design with the performance of PB-LAD. Experimental results show that our technique TB-LAD reduces inter-LA traffic 27 to 36 percent on the average over PB-LAD. TB-LAD outperforms PB-LAD when the average cell sizes are larger than 2,000 meters and the average number of cells in an LA is larger than nine. For our experiment region, which is an actual metropolitan city, our scheme manages to partition the cells into LAs so successfully that the number of location updates becomes almost zero when the LA size is larger than 13 cells and the cell size is larger than 2,500 meters.

## ACKNOWLEDGMENTS

This work is supported in part by the US National Science Foundation under grant number CCR-99-88532.

## REFERENCES

[1] I.F. Akyildiz, J. McNair, J.S.M. Ho, H. Uzunalioglu, and W. Wang, "Mobility Management in Next Generation Wireless Systems," *Proc. IEEE,* vol. 87, no. 8, pp. 1347-1385, Aug. 1999.

[2] I.F. Akyildiz and W. Wang, "A Dynamic Location Management Scheme for Next-Generation Multitier PCS Systems," *IEEE Trans. Wireless Comm.,* vol. 1, no. 1, pp. 178-189, Jan. 2002.

[3] L.P. Araujo and J.R.B. de Marca, "Paging and Location Update Algorithms for Cellular Systems," *IEEE Trans. Vehicular Technology,* vol. 49, no. 5, pp. 1606-1614, Sept. 2000.

[4] H.-W. Hwang, M.-F. Chang, and C.-C. Tseng, "A Direction Based Location Update Scheme with a Line-Paging Strategy for PCS Networks," *IEEE Comm. Letters,* vol. 4, no. 5, pp. 149-151, May 2000.

[5] J. Li, H. Kameda, and K. Li, "Optimal Dynamic Mobility Management for PCS Networks," *IEEE/ACM Trans. Networking,* vol. 8, no. 3, pp. 319-327, June 2000.

[6] Y.-B. Lin, "Reducing Location Update Cost in a PCS Network," *IEEE/ACM Trans. Networking,* vol. 5, no. 1, pp. 25-33, June 1997.

[7] U. Madhow, M.L. Honig, and K. Steiglitz, "Optimization of Wireless Resources for Personal Communications Mobility Tracking," *IEEE/ACM Trans. Networking,* vol. 3, no. 6, pp. 698-707, Dec. 1995.

[8] C.H. Papadimitriu and K. Steiglitz, *Combinatorial Optimization: Algorithms and Complexity.* Prentice Hall, 1987.

[9] C.U. Saraydar, O.E. Kelly, and C. Rose, "One-Dimensional Location Area Design," *IEEE/ACM Trans. Networking,* vol. 49, no. 5, pp. 1626-1632, Sept. 2000.

[10] S. Tabbane, "An Alternative Strategy for Location Tracking," *IEEE J. Selected Areas in Comm.,* vol. 13, no. 5, pp. 880-892, June 1995.

[11] K. Wang, J.-M. Liao, and J.-M. Chen, "Intelligent Location Tracking Strategy in PCS," *IEE Proc. Comm.,* vol. 147, no. 1, pp. 63-68, Feb. 2000.

[12] W. Wang, I.F. Akyildiz, and G. Stuber, "An Optimal Partition Algorithm for Minimization of Paging Costs," *IEEE Comm. Letters,* vol. 5, no. 2, pp. 42-45, Feb. 2001.

[13] V.W.-S. Wong and V.C.M. Leung, "Location Management for Next-Generation Personal Communications Networks," *IEEE Network Magazine,* pp. 18-24, Sept./Oct. 2000.

[14] H. Xie, S. Tabbane, and D. Goodman, "Dynamic Location Area Management and Performance Analysis," *Proc. 43rd IEEE Vehicular Technology Conf.,* pp. 533-539, May 1993.

[15] X. Zhang, J. Castellanos, and A. Campbell, "Design and Performance of Mobile IP Paging," *ACM Mobile Networks and Applications,* special issue on modeling analysis and simulation of wireless and mobile systems, vol. 7, no. 2, Mar. 2002.

[16] http://users.ece.gatech.edu/erdal/metropol1.txt, 2003.

**Erdal Cayirci** (M'97) graduated from the Turkish Army Academy in 1986. He received the MS degree from the Middle East Technical University and the PhD degree from Bogazici University in computer engineering in 1995 and 2000, respectively. He was a visiting researcher with the Broadband and Wireless Networking Laboratory and a visiting lecturer with the School of Electrical and Computer Engineering at Georgia Institute of Technology in 2001. He is director of the Combat Models Operations Department at the Turkish War Colleges Wargaming and Simulation Center and a faculty member with the Department of Computer Engineering at Istanbul Technical University. His research interests include sensor networks, mobile communications, tactical communications, and military constructive simulation. He is an editor for *AdHoc Networks* and guest edited two special issues for *Computer Networks* and *Kluwer Journal on Special Topics in Mobile Networking and Applications* (MONET). He was the program cochair of the First IEEE Sensor Network Protocols and Applications (SNPA) Workshop in 2003. He is a member of the IEEE.

**Ian F. Akyildiz** (M'86-SM'89-F'96) received the BS, MS, and PhD degrees in computer engineering from the University of Erlangen-Nuernberg, Germany, in 1978, 1981, and 1984, respectively. Currently, he is the Ken Byers Distinguished Chair Professor with the School of Electrical and Computer Engineering at the Georgia Institute of Technology and director of the Broadband and Wireless Networking Laboratory. His current research interests are in wireless networks, satellite networks, and next generation Internet. He is an editor-in-chief of *Computer Networks* and *AdHoc Networks* and an editor for *ACM-Kluwer Journal of Wireless Networks.* He is a past editor for *IEEE/ACM Transactions on Networking* (1996-2001), *Kluwer Journal of Cluster Computing* (1997-2001), and *ACM-Springer Journal for Multimedia Systems* (1995-2002), as well as for *IEEE Transactions on Computers* (1992-1996). He guest edited more than 10 special issues for various journals in the last decade. He was the technical program chair of the Ninth IEEE Computer Communications Workshop in 1994, for ACM/IEEE MOBICOM'96 (Mobile Computing and Networking Conference), and IEEE INFOCOM'98 (Computer Networking Conference), as well as IEEE ICC 2003 (International Conference on Communications). He was the general chair of the Eighth ACM MobiCom 2002 Conference. Dr. Akyildiz is an ACM fellow (1997). He received the "Don Federico Santa Maria Medal" for his services to the Universidad of Federico Santa Maria in Chile in 1986. He served as a national lecturer for the ACM from 1989 until 1998 and received the ACM Outstanding Distinguished Lecturer Award for 1994. Dr. Akyildiz received the 1997 IEEE Leonard G. Abraham Prize award (IEEE Communications Society) for his paper, entitled "Multimedia Group Synchronization Protocols for Integrated Services Architectures," published in the *IEEE Journal of Selected Areas in Communications* (JSAC) in January 1996. Dr. Akyildiz received the 2002 IEEE Harry M. Goode Memorial award (IEEE Computer Society) with the citation "for significant and pioneering contributions to advanced architectures and protocols for wireless and satellite networking." He is a fellow of the IEEE.